Proc. Natl. Acad. Sci. USA
Vol. 90, pp. 5613–5617, June 1993
Genetics

Lethality induced by a single site-specific double-strand break in a dispensable yeast plasmid

(DNA repair/recombination/cell cycle)

CRAIG B. BENNETT, ALICE L. LEWIS, KRISTIN K. BALDWIN, AND MICHAEL A. RESNICK

Laboratory of Molecular Genetics, National Institute of Environmental Health Sciences, National Institutes of Health, Box 12233, Research Triangle Park, NC 27709

Communicated by Philip C. Hanawalt, December 28, 1992

ABSTRACT **Cells of the yeast *Saccharomyces cerevisiae* are delayed in the G_2 phase of the cell cycle following chromosomal DNA damage. This arrest is *RAD9*-dependent and suggests a signaling mechanism(s) between chromosomal lesions and cell cycling. We examined the global nature of growth inhibition caused by an HO endonuclease-induced double-strand break (DSB) at a 45-bp YZ sequence (from *MAT* YZ) in a non-yeast region of a dispensable single-copy plasmid. The presence of an unrepaired DSB results in cellular death even though the plasmid is dispensable. Loss of cell viability is partially dependent on the *RAD9* gene product. Following induction of the DSB, 40% of *RAD*$^+$ and 49% of *rad9*Δ cells [including both unbudded (G_1) and budded (S plus G_2) cells] did not progress further in the cell cycle. The remaining *RAD*$^+$ cells progressed to form microcolonies (<30 cells) containing aberrantly shaped inviable cells. For the *rad9*Δ mutant, the majority of the remaining cells produced viable colonies accounting for the greater survival of the *rad9*Δ strain. Based on the profound effects of a single nonchromosomal DNA lesion, this system provides a convenient means for studying the signaling effects of a DNA lesion, as well as for designing strategies for modulating cell proliferation.**

Cell cycle progression is inhibited by chromosomal DNA damage, implying an indirect interaction between DNA lesions and genes involved in cell cycling (1). Such an interaction can be seen in *Escherichia coli*, where DNA damage results in a transient cessation of cell cycling that is under the genetic control of the SOS regulon (2, 3). Induced double-strand breaks (DSBs) or their subsequent repair products appear to serve as strong signals for growth inhibition. The biological consequences of ionizing radiation induced and naturally occurring DSBs have been explored in many eukaryotes (4, 5). In the yeast *Saccharomyces cerevisiae*, the major pathway for DSB repair involves a recombinational interaction between the broken molecule(s) and a homologous chromosome or sister chromatid that is dependent on the *RAD52* gene product (6, 7). Unrepaired DSBs, which could result from insufficient time for repair or from lack of an available homologue [i.e., radiation of G_1 haploids or possibly the presence of a diverged homeologous chromosome (8)], lead to the accumulation of cells in the G_2 phase of the cell cycle. This arrest has been shown to be under *RAD9* control in yeast (refs. 1 and 9–11; this study). *RAD9* appears to serve as a "checkpoint" for assessment of chromosomal damage, possibly preventing cell cycle progression into M phase until lesions are repaired. Other types of DNA damage that impede DNA synthesis can also lead to G_2 arrest in yeast (12). In mammalian cells, DNA-damaging agents have been shown to arrest cells in G_1 as well in G_2 (13).

The publication costs of this article were defrayed in part by page charge payment. This article must therefore be hereby marked "*advertisement*" in accordance with 18 U.S.C. §1734 solely to indicate this fact.

While the effects of DNA damage can be categorized as indirect (i.e., cell cycle arrest) or direct (i.e., aneuploidy resulting from chromosome breakage), the relative importance of individual lesions, the processes leading to the effects, and the genetic controls are difficult to establish. A yeast system was therefore designed that could address the relationship of a unique lesion to DNA repair, cell progression, and lethality. The system relies on the induction of a site-specific nonrepairable DSB in a dispensable single-copy plasmid. Surprisingly, this DSB has profound global consequences on cellular growth and metabolism that result in lethality in both *RAD*$^+$ and *rad9*Δ strains.

MATERIALS AND METHODS

Plasmids. The selectable (*TRP1*) single-copy plasmid pGALHOT (pSE271galHO; Fig. 1) with the HO endonuclease fused to the *GAL10* promoter (14) was obtained from F. Heffron. The YZ-CEN plasmid (12.2 kb; Fig. 1) is a modification of the 9.9-kb plasmid YCpTCUP1 containing *TRP1–CEN3–URA3–CUP1–ARS1–amp*^{r}. This plasmid is comparable to that previously reported (15), except that it lacks the *GAL1-10* promoter fused to the centromere and a 3.25-kb simian virus 40 *ori/neo Eco*RI fragment replaces *TRP1*. One of the *Eco*RI sites (distal to the simian virus 40 promoter) was filled in (resulting in the CEN[NoYZ] control plasmid) and a 300-bp *Eco*RI YZ-containing fragment from pCB145 (see below) was subcloned into the remaining *Eco*RI site. This resulted in the positioning of a single YZ junction between large flanking regions of non-yeast DNA.

pCB145 is a derivative of pJS113 (obtained from J. Singer and F. Heffron), containing a 45-bp *MATα* YZ fragment cloned between the *Bam*HI and *Sal* I sites in pUC19. To construct pCB145, the *Pvu* II fragment from pJS113 was reinserted into the *Hin*cII site of pUC19.

gal::CEN[NoYZ] was derived from CEN[NoYZ] by replacing the *Bam*HI fragment spanning *CEN3* with a *Bam*HI gal::CEN3 fragment from the plasmid pR285 obtained from K. Bloom (16). A 300-bp *Eco*RI fragment from pCB145 was then inserted at the remaining *Eco*RI site to produce the YZ-gal::CEN plasmid.

Strains. The nonswitching *RAD*$^+$ haploid strain tNR85T1 [*ho HMLα leu2 mat::LEU2 hmr-Δ3 mal2 ura3-52 thr4 trp1 GAL*] (17) was transformed (18) with the appropriate plasmids and maintained on synthetic complete (SC) medium (19) containing 2% glucose (+glc) and lacking tryptophan (−trp) and uracil (−ura). The isogenic *rad9*Δ strain was constructed by transforming tNR85T1 with a *Sal* I/*Eco*RI digest of the *RAD9* disruption plasmid pRR330 obtained from R. Schiestl (10). Ura$^+$ transformants were confirmed as *rad9* disruptions by increased sensitivity to UV irradiation and by Southern blotting. One isolate was plated to medium containing 5-fluoroorotate, and a Ura$^-$ colony that retained sensitivity to UV irradiation was transformed with the appropriate plasmids.

Abbreviation: DSB, double-strand break.

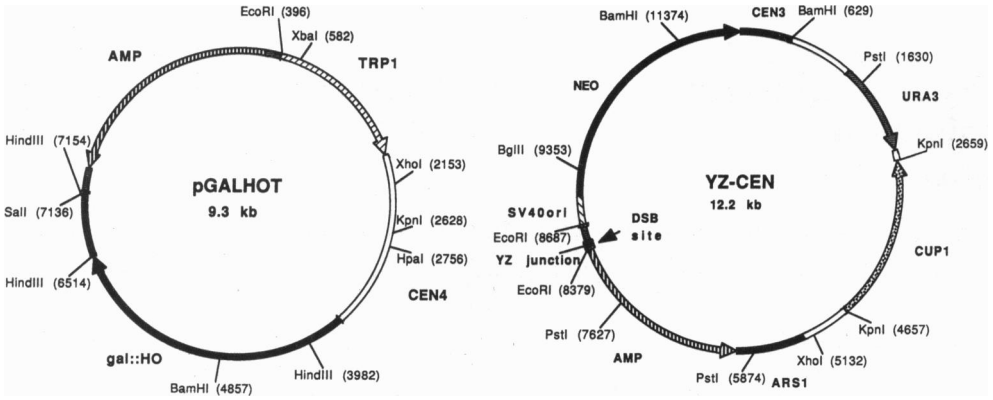

FIG. 1. Production of an unrepaired DSB in a dispensable yeast plasmid. The centromere-containing plasmids are maintained with selection in a nonswitching *GAL*$^+$ yeast strain in the presence of glucose. Galactose induction of the HO endonuclease within pGALHOT produces a unique site-specific DSB at the YZ junction in the YZ-CEN target plasmid. SV40ori, simian virus 40 origin of replication.

Growth and Plating Conditions. Logarithmically growing cells were obtained by inoculating single colonies from SC−trp−ura plates into 10 ml of SC+glc−trp−ura. Cells were grown to 1–3 × 10^7 per ml with vigorous shaking at 30°C. Cells were then washed twice, diluted in sugarless medium, and plated to SC−trp with 2% glucose (glc) or galactose (gal) containing or lacking uracil to select for the target plasmid. Plating efficiency in the presence of the DSB was determined by relative colony formation on gal+ura vs. glc+ura. Plasmid loss was determined by the relative plating efficiencies on glc+ura vs. glc−ura.

Physical Analysis of Site-Specific Plasmid Breakage. Cells were pregrown to 3–5 × 10^7 per ml in glucose medium, washed in medium lacking sugar, suspended in SC−trp+ura+gal, and incubated at 30°C with vigorous shaking. Plasmid DNA from *RAD*$^+$ and *rad9*Δ cells was extracted (20) and separated in 0.7% agarose gels as either unrestricted or *Xho* I-restricted plasmid. Plasmid DNA was visualized after Southern blotting to nylon membranes and probing with digoxigenin-labeled YZ-CEN DNA.

Cell Staining. Cells containing pGALHOT and either YZ-CEN or CEN[noYZ] were grown in galactose medium for 6 hr as described above for Southern blotting. Cells in medium were fixed and stained in a 1:1 ratio (vol/vol) with a freshly prepared 4′,6-diamidino-2-phenylindole solution (5 μl of a 10-μg/ml solution in water mixed with 95 μl of 95% ethanol) and photographed with fluorescence microscopy.

Physical Analysis of Chromosomes. Cells were pregrown to 5 × 10^7 per ml in glucose medium with plasmid selection, washed, and incubated with galactose as described above. Cells were gently lysed in agarose plugs (21) and chromosomes were separated in 1% agarose gels by a Beckman GeneLine II pulsed-field gel apparatus.

RESULTS

Induction of HO Endonuclease Results in a Site-Specific DSB at the Plasmid YZ Junction. DSBs are repaired by recombination in yeast (4–6). To study the global consequences of an unrepaired DSB, we developed a system whereby a single DSB could be induced in a nonessential single-copy (CEN) plasmid under conditions that would inhibit recombination. We utilized the YZ junction of the *MAT* switching locus from *S. cerevisiae* and the YZ site-specific endonuclease HO (14, 22, 23). A 45-bp YZ junction fragment that is sufficient for HO-mediated *in vitro* DSB cleavage was synthesized (24) and inserted between large nonhomologous blocks (3.3 and 2.6 kb) of bacterial DNA contained in a centromere-containing shuttle vector, YZ-CEN. The lack of DNA homology flanking the YZ junction prevents recombinational repair of the DSB. This plasmid and the corresponding control plasmid lacking the YZ junction, CEN[NoYZ], were transformed into nonswitching (deleted at *MAT*) isogenic *RAD*$^+$ and *rad9*Δ haploid strains containing a second centromere plasmid (pGALHOT) with the HO endonuclease gene fused to the galactose-inducible *GAL1-10* promoter (14, 17, 22, 23).

We examined the kinetics and extent of cleavage at the 45-bp YZ target following the transfer of logarithmically growing cells from glucose- to galactose-containing liquid medium. Linearized YZ-CEN plasmid could be detected as early as 2 hr after galactose addition (Fig. 2*A*); maximum cutting was observed in the *RAD*$^+$ strain between 6 and 8 hr. The kinetics of cutting at the YZ junction was delayed slightly in the *rad9*Δ strain; linearization was first detected at 4 hr and maximal cutting occurred between 8 and 10 hr (Fig. 3*B*). Most of the YZ-CEN plasmid was cut at these times (Figs. 2 and 3). From the genetic evidence described below and the loss of detectable plasmid on Southern blots at 24 hr, we conclude that the plasmid was inactivated in nearly all cells that had both plasmids at time 0.

The cutting was specific to the YZ junction in both *RAD*$^+$ and *rad9*Δ cells, based on the appearance of a 3.25-kb fragment following *Xho* I restriction (Fig. 3). No breaks were observed in control cells containing the CEN[NoYZ] plasmid that were incubated in galactose medium (Fig. 2*B*). Thus, induction of HO endonuclease results in the production of a unique DSB in the target YZ-CEN plasmid.

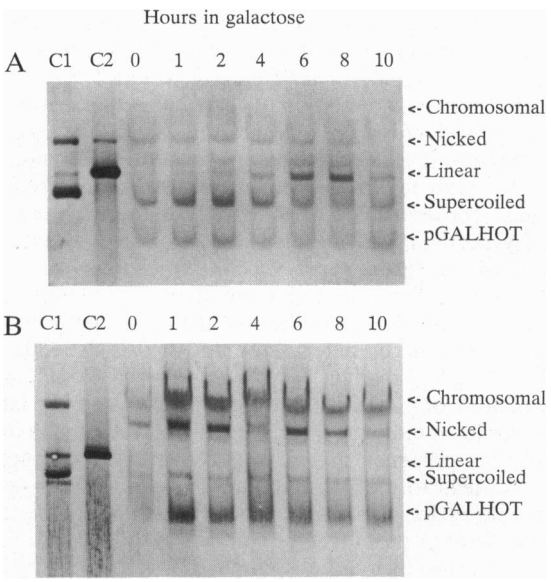

FIG. 2. Production of DSBs in the YZ target plasmid after induction of HO endonuclease. Undigested plasmid DNA was extracted from galactose-induced *RAD*$^+$ cells containing pGALHOT and either YZ-CEN (*A*) or CEN[NoYZ] (*B*) and analyzed by Southern blotting. Positions of nicked, linear, and supercoiled plasmid were estimated by loading 0.1 μg of uncut (lane C1) or *Xho* I-cut (lane C2) control YZ-CEN plasmid DNA. Positions of cross-hybridizing supercoiled pGALHOT plasmid and high molecular weight chromosomal DNA are indicated.

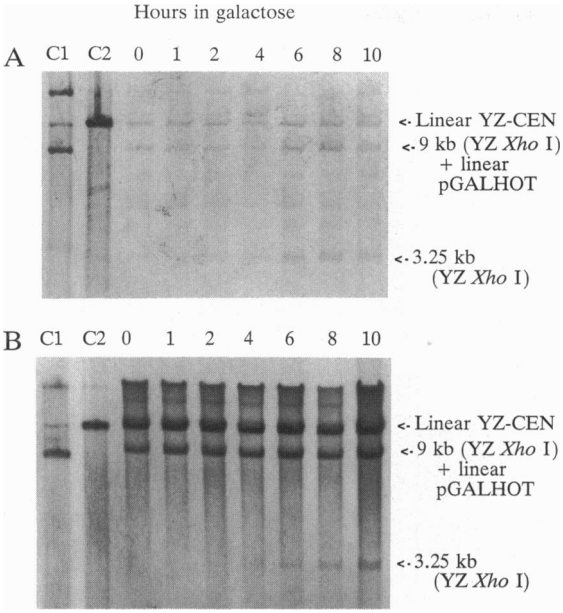

FIG. 3. Production of site-specific DSBs at the plasmid YZ target sequence after induction of HO endonuclease in *RAD*$^+$ (*A*) and *rad9*Δ (*B*) cells. Plasmid DNA was extracted from galactose-induced cells and digested with *Xho* I for Southern blot analysis. Release of 3.25- and 9.0-kb fragments by *Xho* I digestion indicates site-specific plasmid cleavage by HO endonuclease. Linearization of the pGALHOT plasmid by *Xho* I results in a cross-hybridizing 9.3-kb band that migrates at the same position as the 9.0-kb YZ-CEN fragment. Control cells with the CEN[NoYZ] plasmid did not reveal the 3.25-kb fragment after HO induction (data not shown). Position of linear YZ-CEN plasmid was estimated by loading 0.1 μg of uncut (lane C1) or *Xho* I-cut (lane C2) control YZ-CEN plasmid DNA.

A DSB Is Lethal in a Dispensable Plasmid. Even though the YZ-CEN plasmid is dispensable, induction of the DSB greatly reduced cell survival. The relative plating efficiency (glc+ura vs. gal+ura) of YZ-CEN bearing RAD$^+$ cells was 0.10 as compared to 0.58 for cells containing the CEN[NoYZ] plasmid (Table 1). The relative plating efficiency on medium lacking uracil was 100-fold lower (0.0011), suggesting the loss of YZ-CEN plasmid in virtually all cells containing pGALHOT. The estimated survival (corrected for plasmid loss and plating efficiency of control cells on gal+ura) of YZ-CEN cells on gal+ura was 0.15. The survivors were largely (>95%) Ura$^-$, consistent with loss of the YZ-CEN target plasmid, whereas >90% of the colonies that arose from CEN[NoYZ] plasmid-bearing cells were Ura$^+$.

Table 1. Plating efficiency in cells induced for HO endonuclease

Cells	Uracil	CEN[NoYZ]	YZ-CEN	Estimated survival
RAD$^+$	+	0.58	0.1	0.15
	−	0.51	0.0011	—
*rad9*Δ	+	0.73	0.22	0.30
	−	0.66	<0.0016	—

RAD9 and *rad9*Δ cells containing pGALHOT and either YZ-CEN or CEN[NoYZ] plasmids were grown and plated as described in *Materials and Methods*. Colonies were counted after incubation at 30°C for 72 hr. Plating efficiency was determined from the number of colonies arising on glucose vs. galactose plates. Survival was estimated from the relative plating efficiency of YZ-CEN-containing cells vs. CEN[NoYZ]-containing cells after correction for cells lacking the *URA3* target plasmid and therefore unable to produce a plasmid DSB. The percentage of *RAD*$^+$ and *rad9*Δ cells lacking YZ-CEN was 9% and 1%, respectively, based on plating to glucose plates with or without uracil. For the *rad9*Δ strain the 0.30 estimated survival was determined as (0.22)(0.99)/0.73.

The relative plating efficiency on gal+ura following induction of the DSB in the *rad9*Δ mutant was also reduced (0.22) when compared with the CEN[NoYZ] control (0.73; Table 1). While the *rad9*Δ mutant also exhibited a higher estimated survival than the RAD$^+$ strain (0.30 vs. 0.15), most of the lethality due to the DSB was *RAD9*-independent (Table 1).

Differences in nuclear morphology were seen between the *rad9*Δ mutant and the *RAD*$^+$ strain following induction of the DSB. Many (45%) *RAD*$^+$ cells accumulated at G_2 with the nucleus at or within the bud isthmus (Fig. 4*A*), in a manner identical to that seen for γ-irradiated cells (1). Since many of these cells went on to form microcolonies (Fig. 5), cell cycle blockage at G_2 was transient. Cells with the CEN[NoYZ] plasmid (Fig. 4*B*) were distributed throughout the cell cycle, as expected for logarithmically growing cells. The *rad9*Δ cells differed in that there was no accumulation of G_2 cells after induction of the DSB. However, 80% of the cells were enlarged and many were elongated and contained large vacuoles (Fig. 4*E*). Sixty-five percent of the cells also contained enlarged diffuse nuclei lacking clear definition, some with multiple fluorescent centers (Fig. 4*C*) (from their size, these do not correspond to mitochondrial DNA). The control *rad9*Δ cells (carrying the CEN[NoYZ] plasmid) had single compact nuclei with well-defined margins (Fig. 4 *D*) and were not enlarged (Fig. 4*F*).

Inhibition of Cell Progression by a DSB. To address the long-term cellular consequences of the DSB, individual cells from a logarithmically growing culture were examined microscopically up to 48 hr after plating to gal+ura medium (Fig. 5). *RAD*$^+$ or *rad9*Δ cells were located microscopically and classified (1) as "single" (in the G_1 phase of the cell cycle), "budded" (with a small bud; in S phase), or "doublet" (with a bud more than half the size of the mother cell; corresponding to G_2). Since budded and doublet cells responded similarly, these two categories were pooled and presented as budded in Fig. 5.

Many of the *RAD*$^+$ and *rad9*Δ cells carrying YZ-CEN did not grow following DSB induction. Of the cells initially plated to galactose medium (both single, Fig. 5*A*, and budded, Fig. 5*B*), 40% of the *RAD*$^+$ and 49% of the *rad9*Δ cells retained their initial morphology. The remainder progressed to form small or large microcolonies. By comparison, only 14% (*RAD*$^+$) and 15% (*rad9*Δ) of the cells containing the CEN[NoYZ] plasmid (Fig. 5) did not progress; the remainder gave rise to large viable microcolonies (>30 cells). Thus, there is a *RAD9*-independent inhibition of growth that does not depend on the cell cycle stage at the time of plating.

Small-Microcolony Formation in Response to a DSB Is *RAD9*-Dependent. Of the *RAD*$^+$ cells plated to gal+ura and containing the YZ-CEN plasmid, 50% progressed to form small (3–30 cells) microcolonies (Fig. 5). Only 10% of *rad9*Δ cells progressed to form small microcolonies. Most of the *rad9*Δ cells that did not arrest as single or budded cells proceeded to form large (>30 cells) viable microcolonies. This accounted for the increased survival when compared with *RAD*$^+$ (Table 1). Further, cells within the *RAD*$^+$ microcolonies produced an aberrant filamentous morphology not seen in the *rad9*Δ microcolonies (Fig. 4 *G* and *H*). The observation of altered cell morphology and decreased division in the microcolonies of *RAD*$^+$ but not *rad9*Δ mutants suggests a long-term *RAD9*-dependent effect on cell growth following induction of the DSB.

A DSB Results in a Lethal Arrest of Individual Cells and Microcolonies. A surprising effect of the DSB in the *RAD*$^+$ strain was that it could have a long-term lethal effect even in those cells that went on to give rise to microcolonies. The frequency of small microcolonies (3–30 cells; Fig. 5) was higher than the estimated survival of *RAD*$^+$ cells (45% vs. 15%, respectively; Table 1), indicating that all of the cells within most microcolonies were inviable. To test this, single

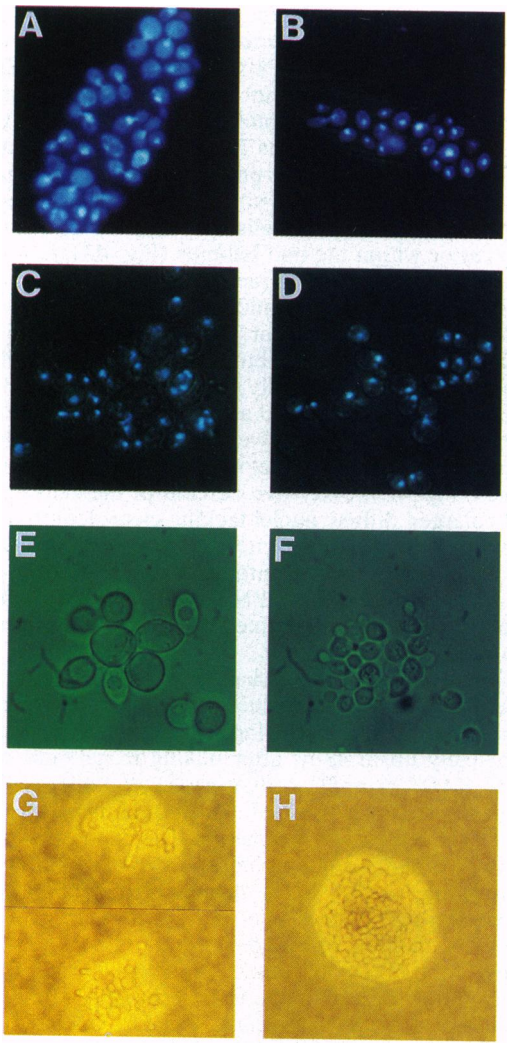

FIG. 4. Morphology of *RAD*$^+$ and *rad9*Δ cells containing a DSB. (*A*) *RAD*$^+$ cells containing YZ-CEN were grown in galactose for 6 hr to induce extrachromosomal DSBs. Cells in medium were fixed and stained with 4′,6-diamidino-2-phenylindole and photographed with fluorescence microscopy. Many of the cells arrested as enlarged "dumbbells" with the nucleus at or within the bud neck, indicating G_2 arrest. (×760.) (*B*) *RAD*$^+$ control cells containing CEN[NoYZ] were grown in galactose, fixed, stained, and photographed as for *A*. Few cells exhibit a G_2/M morphology. The majority of the cells are single (G_1) with compact and distinct fluorescent nuclei. (×760.) (*C*) *rad9*Δ cells containing YZ-CEN were grown, fixed, and stained as above and photographed by combined visible and fluorescence microscopy. Many of the cells are enlarged with diffuse nuclei, and some exhibit multiple fluorescent centers. There is no accumulation of cells in G_2 as observed for *RAD*$^+$ cells. (×1200.) (*D*) *rad9*Δ control cells containing CEN[NoYZ] were grown in galactose, fixed, stained, and photographed as for *C*. Cells are at various positions in the cell cycle similar to the *RAD*$^+$ control cells seen in *B*. (×1200.) (*E*) *rad9*Δ cells containing YZ-CEN were grown, fixed, and stained as above and photographed with visible microscopy. A majority of the cells are greatly enlarged, each containing a large vacuole. (×1200.) (*F*) *rad9*Δ control cells containing CEN-[NoYZ] were grown in galactose, fixed, stained, and photographed as for *E*. Control cells are small (as compared with those in *E*) and without vacuoles. (×1200.) (*G*) Nonviable microcolonies of *RAD*$^+$ cells containing YZ-CEN after 48 hr of growth at 30°C on an SC−trp+ura+gal plate. Colonies that arise from *RAD*$^+$ cells containing CEN[NoYZ] under similar growth conditions contain thousands of cells, are not filamentous or elongated, and are viable. (×960.) (*H*) Microcolony of *rad9*Δ cells containing YZ-CEN after 48 hr of growth at 30°C on an SC−trp+ura+gal plate. Cells within microcolonies are viable with morphology similar to that of *RAD*$^+$ or *rad9*Δ controls. (×960.)

cells or microcolonies from sectioned galactose plates were transferred to nonselective nutrient-rich medium containing

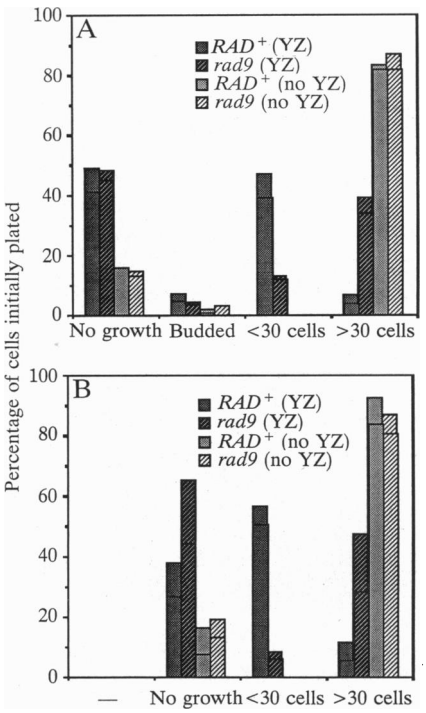

FIG. 5. Inhibition of cell progression of *RAD*$^+$ and *rad9*Δ cells by a plasmid DSB. Cells were grown and washed as described for Table 1 and sonicated briefly on ice to separate cells prior to plating. Cells were plated to SC+gal−trp+ura by using a 48-pin plating device (15). The growth progression of individual single (G_1) (*A*) or budded (S plus G_2) (*B*) cells was determined microscopically after 48 hr at 30°C. In *A* are G_1 cells that either remained as initially plated (no growth) or progressed into budded cells, small microcolonies (<30 cells), or large microcolonies (>30 cells). In *B* are budded cells (S plus G_2), that remained as initially plated (no growth) or progressed to small (<30 cells) or large (>30 cells) microcolonies. The upper and lower horizontal bars within each column corresponds to the results from two independent experiments. In each experiment 200–250 cells were examined. For the two experiments at time 0 the *RAD*$^+$ populations had an average of 59% G_1, 24% S, and 17% G_2 cells and the *rad9*Δ populations had an average of 65% G_1, 25% S, and 10% G_2.

glucose (YEPD) in order to turn-off the HO endonuclease. After incubation for another 3 days, the number of viable colonies arising from the single cells and microcolonies was determined. Microcolonies containing >30 cells always yielded large viable macrocolonies, whereas the single and budded cells as well as the cells contained within the small (<30 cells) microcolonies were incapable of growth. Thus the long-term responses of *RAD*$^+$ cells can be divided into two categories: *RAD9*-independent lethal cell arrest and *RAD9*-dependent limited growth followed by lethal cell arrest.

Recombination Between Chromosomes and the YZ-CEN Plasmid Is Not Observed. Recombinational repair of the broken YZ-CEN plasmid might account for the observed lethality if it led to the formation of a dicentric chromosome. The plasmid centromere was therefore replaced by *CEN3* to which a galactose-inducible *GAL1-10* promoter was fused (16), rendering the centromere nonfunctional in galactose. If lethality were resulting mainly from plasmid integration and dicentric formation, cell viability would be restored on galactose (when compared to YZ-CEN), and dicentric colonies arising on galactose plates would not grow on glucose due to restoration of centromere function. When *RAD*$^+$ cells containing pGALHOT and the YZ-gal::CEN plasmid were plated to gal−ura, the survival was comparable to that observed with the YZ-CEN plasmid (<0.2%), suggesting that dicentrics were rare in the population. Further, none (0/304) of the colonies arising on gal+ura were Ura$^+$, and upon

replating to glucose there was no loss in colony viability. This indicates that integration does not occur for either the YZ-gal::CEN or, presumably, the YZ-CEN plasmid.

We further examined whether plasmid degradation (from the YZ junction to the plasmid yeast marker *CEN3, URA3*, or *CUP1*) might lead to a "one-ended" recombination event, thereby fragmenting the chromosome at the position of the homologous chromosomal gene. Following induction of the DSB, whole chromosomes were characterized by gel electrophoresis and probed with digoxigenin-labeled YZ-CEN sequences. There was no evidence of reduction in size of the relevant chromosomes up to 24 hr after incubation with galactose (data not shown). As expected, there was no HO-mediated cleavage of chromosome III at the intact *HML* locus.

A "one-ended" recombination event mediated by recombination between the bacterial *amp* sequence of the YZ-CEN plasmid with that of the pGALHOT plasmid could result in loss of the *TRP1* marker and cell death due to tryptophan starvation. Maintenance of pGALHOT was unaffected by incubation (up to 24 hr) of YZ-CEN cells in galactose medium with or without selection for the plasmid.

DISCUSSION

A single nonchromosomal DSB that is not subject to repair can have severe consequences on cellular growth and metabolism leading to lethality in *RAD*$^+$ cells. The lethality is not due to loss of genetic information, since the selection for plasmid information was removed at the time of DSB induction. This result suggests a mechanism for dominant lethality that has been described for x-irradiated *rad52* cells, which are deficient in DSB repair (25). The mechanism of DSB-induced dominant lethality may involve cellular signaling processes mediated by kinases and/or phosphatases with multiple intracellular targets such as the cell cycle, segregation, replication, or recombination apparatus.

There appear to be *RAD9*-independent and -dependent lethal responses to the DSB. The frequency of cells that die without growth is comparable for the *rad9*Δ and *RAD*$^+$ cells. This implies that there may be additional genetically identifiable control(s) on cell growth in response to DNA damage that is not related to a specific stage of the cell cycle. Such stage-independent DSB-mediated lethality has been observed for eukaryotic cells undergoing apoptosis (26, 27).

The importance of the *RAD9* gene product in the response to the DSB was evident in those cells capable of cell progression. Among the cells that continued to cycle, the *RAD9* gene was responsible for a G_2/M delay (Fig. 4), thereby sensing the DSB in a manner similar to radiation-induced chromosomal damage (1, 9–11). The *RAD9* gene product is also required for the development of small microcolonies containing inviable cells that contribute to the low survival of *RAD*$^+$ cells in response to the DSB (Table 1 and Fig. 5). The mechanism of this *RAD9*-dependent DSB-induced delayed lethality is not clear. Possibly the DSB-induced signal can be transmitted to subsequent generations and/or the broken plasmid continues to replicate for a limited number of generations. There also appear to be cellular and nuclear morphology differences in the *rad9*Δ vs. the *RAD*$^+$ strain following DSB induction, suggesting a role for the *RAD9* gene product in cellular metabolism immediately following DNA damage (Fig. 4). Another gene, *RNC1*, has also been examined because of a proposed role in *RAD52*-mediated recombination (E. Perkins and M.A.R., unpublished work), and conserved sequence homology with GTP-binding proteins (28), suggests a possible signaling function. Recent results indicate that deletion of *RNC1* suppressed the lethal effects of the plasmid-borne DSB (C.B.B. and M.A.R., unpublished work), suggesting that *RNC1* may play a central role in the DSB signaling responses, including growth arrest.

While there has been substantial progress in characterizing the molecular and genetic control of the yeast cell cycle (29, 30), little is known about the cell cycle response to DNA damage or the signaling mechanisms. However, replication and/or processing of the ends of a DSB are likely to figure prominently. A signal could result from the exposure of single-stranded DNA as proposed for the activation of the SOS regulon of *E. coli*, resulting in cell division arrest following DNA damage (2, 31). For chromosomal *MAT* YZ junctions that have been cut, 5′ → 3′ exonuclease digestion of one strand has been detected (32, 33). The 5′ → 3′ processing of double-stranded ends could act indirectly in DSB recombinational repair by signaling a growth arrest to allow time for repair prior to M phase, as well as directly by providing an invasive 3′ end (6).

Understanding the molecular mechanism(s) of the lethal arrest caused by a nonchromosomal DNA lesion and elucidation of the genetic control(s) for this pathway should provide insights into eukaryotic DNA repair, recombination, and cell cycle regulation. In addition, this system may provide opportunities for designing strategies to modulate the effects of DNA-damaging agents, including the limitation of uncontrolled cell proliferation.

We gratefully acknowledge the suggestions and comments of Ted Weinert, Lee Hartwell, Paul Nurse, Kerry Bloom, Jim Mason, Ed Perkins, Kevin Lewis, and Miro Radman; assistance with chromosome analysis by Jim Westmoreland; strains and plasmids from James Haber and Fred Heffron; and preparation of Fig. 1 by Greg Porter.

1. Weinert, T. A. & Hartwell, L. H. (1988) *Science* **241**, 317–322.
2. Walker, G. C. (1984) *Microbiol. Rev.* **48**, 60–93.
3. Lutkenhaus, J. (1990) *Trends Genet.* **6**, 22–25.
4. Szostak, J. W., Orr-Weaver, T. L., Rothstein, R. J. & Stahl, F. W. (1983) *Cell* **33**, 25–35.
5. Thaler, D. & Stahl, F. (1988) *Annu. Rev. Genet.* **22**, 169–197.
6. Resnick, M. A. (1976) *J. Theor. Biol.* **59**, 97–106.
7. Orr-Weaver, T. L. & Szostak, J. W. (1985) *Microbiol. Rev.* **49**, 33–58.
8. Resnick, M. A., Skaanild, M. & Nilsson-Tillgren, T. (1989) *Proc. Natl. Acad. Sci. USA* **86**, 2276–2280.
9. Hartwell, L. H. & Weinert, T. A. (1989) *Science* **246**, 629–634.
10. Schiestl, R. H., Reynolds, P., Prakash, S. & Prakash, L. (1989) *Mol. Cell. Biol.* **9**, 1882–1896.
11. Weinert, T. A. & Hartwell, L. H. (1990) *Mol. Cell. Biol.* **10**, 6554–6564.
12. Kupiec, M. & Simchen, G. (1985) *Mol. Gen. Genet.* **201**, 558–564.
13. Kastan, M. B., Onyekwere, O., Sidransky, D., Vogelstein, B. & Craig, R. (1991) *Cancer Res.* **51**, 6304–6311.
14. Kostriken, R. & Heffron, F. (1984) *Cold Spring Harbor Symp. Quant. Biol.* **49**, 89–96.
15. Resnick, M. A., Westmoreland, J. & Bloom, K. (1990) *Chromosoma* **99**, 281–288.
16. Hill, A. & Bloom, K. (1989) *Mol. Cell. Biol.* **9**, 1368–1370.
17. Rudin, N. & Haber, J. E. (1988) *Mol. Cell. Biol.* **8**, 3918–3928.
18. Schiestl, R. H. & Gietz, R. D. (1989) *Curr. Genet.* **16**, 339–346.
19. Whittaker, S., Rockmill, B. M., Blechel, A. E., Malone, D. H., Resnick, M. A. & Fogel, S. (1988) *Mol. Gen. Genet.* **215**, 10–18.
20. Hoffman, C. S. & Winston, F. (1987) *Gene* **57**, 267–272.
21. Schwartz, D. C. & Cantor, C. R. (1984) *Cell* **37**, 67–75.
22. Nickoloff, J. A., Chen, E. Y. & Heffron, F. (1986) *Proc. Natl. Acad. Sci. USA* **83**, 7831–7835.
23. Strathern, J. N., Klar, A. J. S., Hicks, J. B., Abraham, J. A., Ivy, J. M., Nasmyth, K. A. & McGill, C. (1982) *Cell* **31**, 183–192.
24. Nickoloff, J. A., Singer, J. D., Hoekstra, M. F. & Heffron, F. (1989) *J. Mol. Biol.* **207**, 527–541.
25. Ho, K. S. Y. & Mortimer, R. K. (1973) *Mutat. Res.* **20**, 45–51.
26. Williams, G. T. (1991) *Cell* **65**, 1097–1098.
27. Barry, M. A., Behnke, C. A. & Eastman, A. (1990) *Biochem. Pharmacol.* **40**, 2353–2362.
28. Chow, T. Y.-K., Perkins, E. L. & Resnick, M. A. (1992) *Nucleic Acids Res.* **20**, 5215–5221.
29. Reed, S. I. (1991) *Trends Genet.* **7**, 95–99.
30. Pringle, J. R. & Hartwell, L. H. (1981) in *The Molecular Biology of the Yeast Saccharomyces*, eds. Strathern, J., Jones, E. & Broach, J. (Cold Spring Harbor Lab. Press, Plainview, NY), pp. 97–142.
31. Sassanfar, M. & Roberts, J. W. (1990) *J. Mol. Biol.* **212**, 79–96.
32. White, C. I. & Haber, J. E. (1990) *EMBO J.* **9**, 663–673.
33. Sugawara, N. & Haber, J. (1992) *Mol. Cell. Biol.* **12**, 563–575.